Electronic Supplementary Material (ESI) for Journal of Materials Chemistry A.

Supporting Information

Multi-Functional Perovskite Oxide $Pr_{0.6}Sr_{0.4}Mn_{0.2}Fe_{0.7}Ni_{0.1}O_{3-\delta}$ as an Efficient Quasi-Symmetric Electrode for Solid oxide Fuel/Electrolysis Cells

Junil Choi[a], Daehee Jang[a], Minho Kim[a], Jungseub Ha[a], Hwichan Ahn[a], and Won Bae Kim[a, b, *]

[a] Department of Chemical Engineering, Pohang University of Science and Technology (POSTECH), 77 Cheongam-ro, Nam-gu, Pohang, Gyeongbuk, 37673, Republic of Korea

[b] Graduate Institute of Ferrous & Energy Materials Technology, Pohang University of Science and Technology (POSTECH), 77 Cheongam-ro, Nam-gu, Pohang, Gyeongbuk 37673, Republic of Korea

*Corresponding authors

E-Mail addresses: kimwb@postech.ac.kr

Table S1. Peak power density (PPD) comparison of symmetric electrodes in H_2-operated SOFC

Material	Electrolyte	Cell configuration	PPD ($W\ cm^{-2}$)		Ref
			Gas	Value (Temp.)	
$(La_{0.8}Sr_{0.2})_{0.9}Sc_{0.2}Mn_{0.75}Ru_{0.05}O_{3-\delta}$ (LSCMR)	SSZ (200μm)	LSSMR|SSZ|LSSMR	wet H_2	0.318 (800°C)	[1]
$Sr_2Ti_{0.8}Co_{0.2}FeO_6$ (STCF)	LSGM (270μm)	STC02F|LSGM|STC02F	dry H_2	0.555 (800°C)	[2]
$La_{0.6}Sr_{0.4}Fe_{0.95}Ru_{0.05}O_{3-\delta}$ (LSFRu)	LSGM (300μm)	LSGMR05|LSGM|LSGMR05	dry H_2	602 (850°C)	[3]
$La_{0.5}Sr_{0.5}Fe_{0.9}W_{0.1}O_{3-\delta}$ (LSFW)	LSGM (250μm)	LSFW|LSGM|LSFW	wet H_2	0.618 (800°C)	[4]
$Ce_{0.2}Sr_{0.8}Fe_{0.95}Ru_{0.05}O_3$ (CeSFR)	LSGM (320μm)	Ce20SFR|LSGM|Ce20SFR	dry H_2	0.846 (800°C)	[5]
$Pr_{0.6}Sr_{0.4}Fe_{0.8}Mn_{0.2}O_{3-\delta}$ –$Ce_{0.9}Gd_{0.1}O_{2-\delta}$ (PSMFN-GDC)	LSGM (300μm)	PSMFN-GDC|LSGM|PSMFN-GDC	dry H_2	602 (850°C)	This work

Material	Electrolyte	Cell configuration	Current density (A cm^{-2})		Ref
			Gas	Value (Temp., Voltage)	
$La_{0.4}Sr_{0.6}Co_{0.2}Fe_{0.7}Nb_{0.1}O_{3-\delta}$ (LSCFNb)	YSZ (200µm)	LSCFN-GDC|YSZ|LSCFN-GDC	30% CO/CO_2	0.4 (800℃, 1.5V)	[6]
$La_{0.6}Sr_{0.4}Fe_{0.95}Pt_{0.05}O_{3-\delta}$ (Fe@LSPt)	LSGM (300µm)	LSPt|LSGM|LSPt	50% CO/CO_2	0.65 (850℃, 1.5V)	[7]
$(La,Sr)Fe_{0.9}Ni_{0.1}O_{4+\delta}$ (RPLSFN0.1)	LSGM (300µm)	RPLSFN0.1|LSGM|RPLSFN0.1	50% CO/CO_2	0.75 (800℃, 1.5V)	[8]
$La_{0.8}Sr_{0.2}Cr_{0.5}Fe_{0.5}O_{3-\delta}$-$Zr_{0.84}Y_{0.16}O_{2-\delta}$ (LSCrF-YSZ)	YSZ (200µm)	LSCrF-YSZ|YSZ|LSCrF-YSZ	30% CO/CO_2	0.75 (850℃, 1.5V)	[9]
$La_{0.65}Bi_{0.1}Sr_{0.25}Cr_{0.5}Fe_{0.5}O_{3-\delta}$-$Ce_{0.8}Sm_{0.2}O_{1.9}$ (LBiSCRF-SDC)	LSGM (330µm)	Bi-LSCRF-SDC|LSGM|Bi-LSCRF-SDC	50% CO/CO_2	0.79 (800℃, 1.5V)	[10]
$Pr_{0.6}Sr_{0.4}Fe_{0.8}Mn_{0.2}O_{3-\delta}$-$Ce_{0.9}Gd_{0.1}O_{2-\delta}$ (PSMFN-GDC)	LSGM (300µm)	PSMFN-GDC|LSGM|PSMFN-GDC	30% CO/CO_2	1.02 (850℃, 1.5V)	This work

Table S2. Current density comparison of symmetric electrodes for CO_2 electrolysis in SOEC.

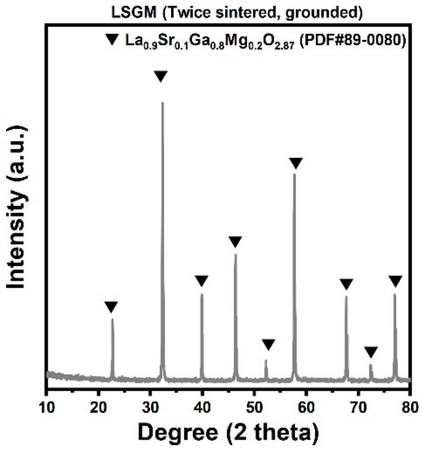

Fig. S1. XRD pattern of grounded twice-sintered LSGM pellet.

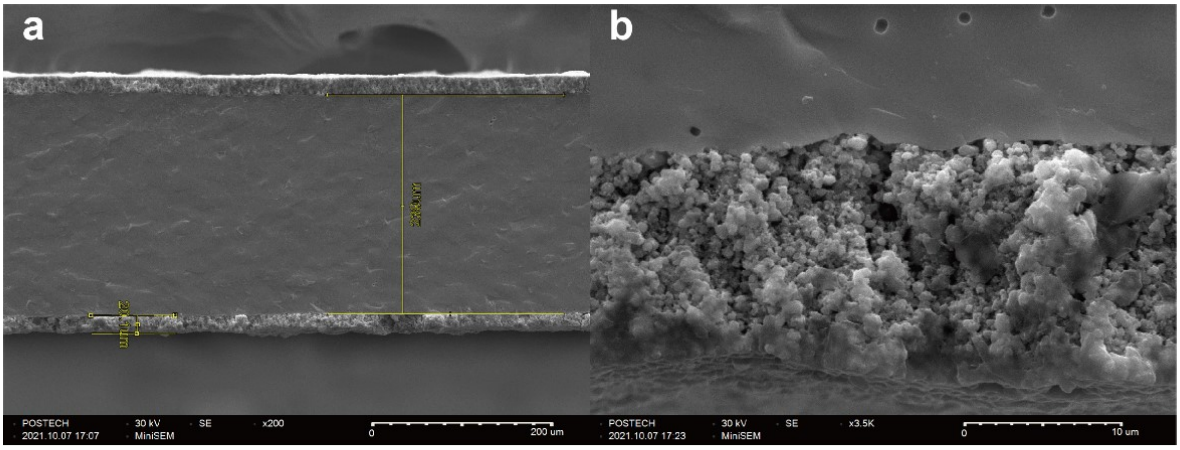

Fig S2. The Cross-sectional SEM images of (a) PSMFN-GDC symmetrical cell based on LSGM electrolyte and (b) magnified electrode.

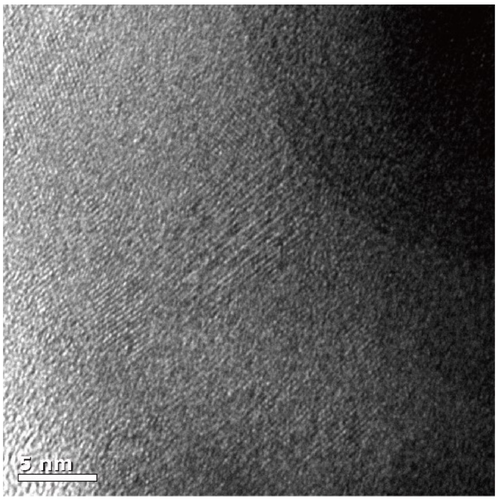

Fig S3. HR-TEM image of reduced PSMFN.

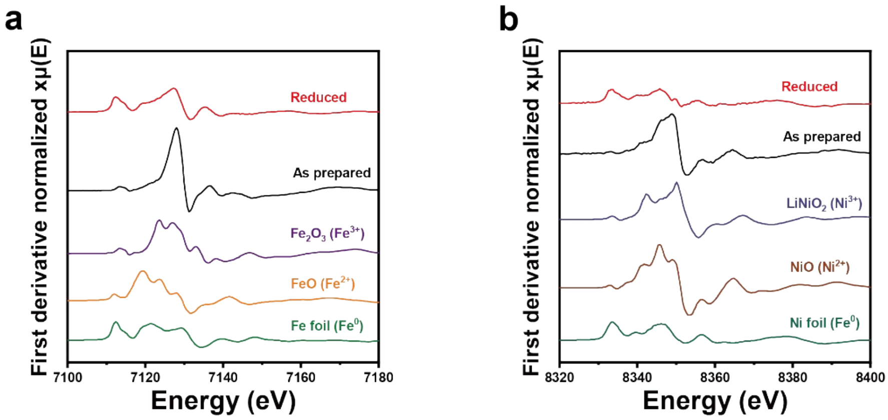

Figure S4. The 1st derivative curves of XAENS spectra of PSMFN, reduced PSMFN and corresponding reference oxides at (a) Fe-K edge and (b) Ni K-edge

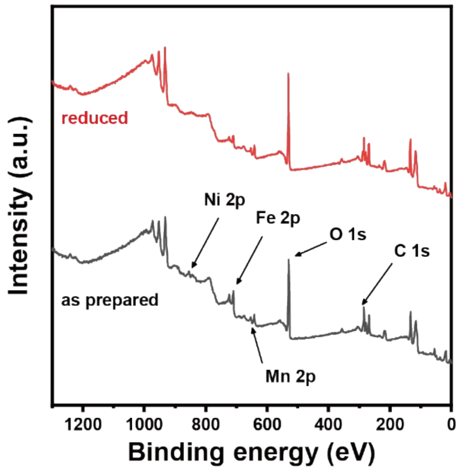

Figure S5. XPS surveys of the as prepared and reduced PSMFN

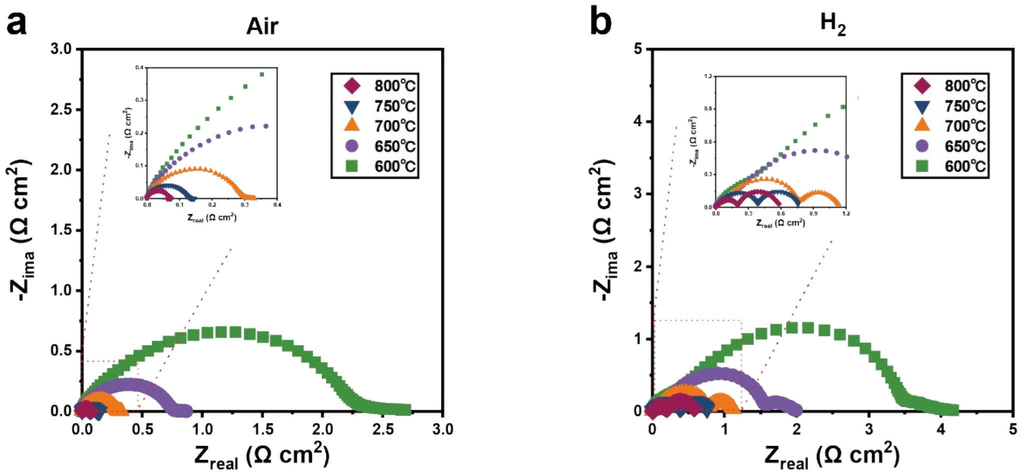

Figure S6. Symmetric half-cell tests of PSMFN-GDC under (a) air and (b) H_2 atmosphere.

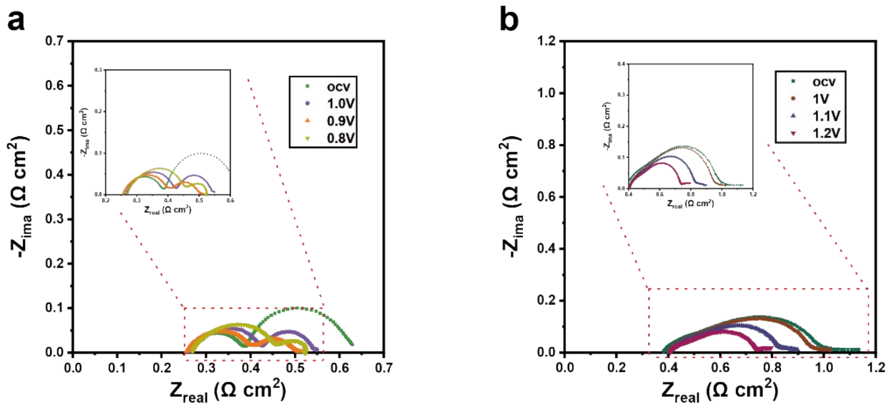

Figure S7. EIS profiles of PSMFN-GDC symmetric cell under applied voltage conditions in (a) SOFC mode and (b) SOEC mode

References

[1] J. Zhou, N. Wang, J. Cui, J. Wang, J. Yang, Z. Zong, Z. Zhang, Q. Chen, X. Zheng, K. Wu, J. Alloys Compd., 2019, **792**, 1132–1140.

[2] B. Niu, C. Lu, W. Yi, S. Luo, X. Li, X. Zhong, X. Zhao, B. Xu, Appl. Catal. B, 2020, **270**, 118842.

[3] M. Marasi, L. Duranti, I. Luisetto, E. Fabbri, S. Licoccia, E. Di Bartolomeo, J. Power Sources, 2023, **555**, 232399.

[4] S. Wang, B. Wei, Z. Lü, Int. J. Hydrogen Energy, 2021, **46**, 30101–30111.

[5] B. Li, S. He, J. Li, X. Yue, J.T.S. Irvine, D. Xie, J. Ni, C. Ni, ACS Catal., 2020, **10**, 14398–14409.

[6] Z. Yang, C. Ma, N. Wang, X. Jin, C. Jin, S. Peng, J. CO2 Util., 2019, **33**, 445–451.

[7] A.P. Panunzi, L. Duranti, I. Luisetto, N. Lisi, M. Marelli, E. Di Bartolomeo, Chem. Eng. J., 2023, **471**, 144448.

[8] C. Liu, C. Sun, L. Bian, W. Yu, J. Qi, S. Li, J. Gao, J. Peng, J. Peng, S. An, Int. J. Hydrogen Energy, 2022, **47**, 9517–9526.

[9] S. Xu, S. Li, W. Yao, D. Dong, K. Xie, J. Power Sources, 2013, **230**, 115–121.

[10] Y. Wan, Y. Yang, Y. Lu, R. Peng, C. Xia, ACS Appl. Energy Mater., 2022, **5**, 2339–2348.